ACCSCIENCE PUBLISHING

Asian Journal of Water, Environment and Pollution. Vol. 22, No. 2 (2025), pp. 64-86.
doi: 10.36922/AJWEP025040019

ORIGINAL RESEARCH ARTICLE

Geospatial flood modeling and risk assessment of floodplain villages along the Barak River, Northeast India

Shanku Ghosh and Chakkaravarthi Prakasam*

Department of Geography, School of Earth Sciences, Assam University Diphu Campus, Karbi Anglong, Assam, India
***Corresponding author:** Chakkaravarthi Prakasam (cprakasam@gmail.com)

Received: January 22, 2025; 1st revised: March 4, 2025; 2nd revised: March 15, 2024; Accepted: March 17, 2025; Published Online: April 4, 2025

Abstract: Floods are events where areas or lands become submerged due to an excessive volume of water, leading to various impacts, such as human casualties; property damage; and social, economic, and environmental losses. This study aims to investigate the factors influencing flood hazard modeling using statistical models (e.g., frequency ratio, Shannon entropy) to identify flood-prone areas and assess the flood risk in villages within the Barak River basin for effective flood management. Among the states in India, Assam, Bihar, Uttar Pradesh, and West Bengal are among those that are highly affected by floods. In Assam, the Barak and Brahmaputra River valleys are particularly vulnerable to flooding, with Barak Valley being extremely prone to flood following monsoonal downpours and breaches in river embankment. This study's findings reveal that the entire Barak River floodplain (Barak Valley) exhibits high to very high flood susceptibility. All districts within Barak Valley show more than 50% of their area as flood-prone, with Karimganj district having the highest flood susceptibility, as 70% of its area is in the very high-risk category, which is the highest among the districts. A total of 866 villages in the study area are highly vulnerable to floods, accounting for 46% of the villages in the region. These villages are mostly located along the riverbanks and low-lying areas surrounding water bodies. These findings emphasize the need for targeted flood management strategies such as forecasting, early warning systems, and land use planning in these villages.

Keywords: Flood hazard; Vulnerability; Exposure risk assessment; Statistical models; Barak River basin

1. Introduction

Global flood risk is a significant concern, with studies showing an increasing trend in flood risk worldwide due to climate change.[1-3] High-income countries, including Singapore, Japan, Luxembourg, and South Korea, are among the most at-risk nations, with a slow but steady rise in flood risk projected under different scenarios.[1] Vulnerability to floods is influenced by exposure, sensitivity, and coping capacity, with spatial disparities between continents highlighting Asia and Europe as high-risk areas.[4] To address the challenges of flood risk assessment in developing regions, we need to map flood hazard, vulnerability, and risk, enabling reliable assessments and strengthening resilience worldwide.[5] Among the different types of disasters, floods are the single largest disaster, causing 21% of total disaster deaths, 13.46% of injuries, 46.73% of the disaster-affected population, and 24.38% of worldwide disaster economic damage.[6] Asia is home to a disproportionate share of 73% of the global flood-risk population. Within Asia, South Asia bears the brunt of flood impacts, with 39% of the continent's flood-affected population residing there, followed by Southeast and East Asia with 30% and 20%, respectively.[7] Globally, India is the second most flood-affected country next to China.[8]

India's climate is characterized by highly unpredictable monsoon rainfall. The country is home to numerous large and small rivers, and prolonged heavy downpours often lead to widespread flooding. India is a global hotspot for flooding. According to the Central Water Commission's 2010 data, roughly 40 million hectares of Indian land are susceptible to inundation, making it the world's second most flood-prone country. Annually, an average of 7.6 million hectares bears the brunt of these floods. Between 1953 and 2009, these floods inflicted a staggering economic toll of approximately 200 billion dollars in damages while tragically claiming the lives of nearly 92,000 people.[9] Flood damage in India varies across states. Bihar, West Bengal, Orissa, Assam, Andhra Pradesh, and Gujarat are highly affected by flooding. In 2018, Kerala faced severe floods, with extensive damage to property, infrastructure, and agriculture, costing approximately Rs. 3000 crores for rebuilding efforts.[10] Maharashtra, particularly districts such as Mumbai, Palghar, Thane, Raigad, Satara, Sangli, Pune, and Kolhapaur, experienced significant flood events in 2019 due to extremely heavy rainfall, emphasizing the importance of mitigation and adaptation strategies.[11] Among all the states in India, 10 states account for 46% of the country's floods, with Uttar Pradesh and Bihar constituting the highest proportion. Notably, 55% of Bihar's geographical area is affected by floods, followed by Assam (50%), Uttar Pradesh (37%), and West Bengal (32%). Physiographically, Assam is primarily divided into two main drainage systems: the Barak Valley and the Brahmaputra Valley. Both river valleys are highly prone to flooding, which is closely linked to the monsoon season. The formation of the monsoonal trough in the hilly and plateaus of Assam leads to huge downpours, resulting in excess accumulation of monsoonal rainfall in the rivers and subsequent flooding in plain areas. Major flooding events in Assam have been a recurring and devastating natural disaster, impacting both life and property in the region. The Brahmaputra River, along with extreme rainfall events in the Arunachal Himalaya, contributes significantly to floods in Assam.[12,13] Dhemaji district[14] and Majuli Island[15] are particularly notable as the worst flood-affected areas in Assam, with a significant portion of land being inundated during flood events. The southwest monsoon of 2019 brought heavy rainfall, leading to severe flooding in Assam, affecting millions of people and causing substantial damage to life and property.[16] These events underscore the urgent need for improved flood forecasting models and effective flood hazard management strategies in Assam to mitigate the impact of such disasters in the future.

The present study focuses on the Barak River, which is highly flood-prone. Each year, during the monsoon season, it inundates the downstream floodplains and causes damage in the Cachar, Karimganj, and Hailakandi districts of Assam. The study aims to develop Barak River flood hazard models and risk assessments for the flood-affected villages.

Modeling and mapping flood hazard zones are essential to flood disaster management. Flood hazard modeling methods are classified into three categories: empirical, physical, and physically-based models. The different types of empirical models are statistical, multi-criteria decision-making (MCDM), and machine learning/artificial intelligence. Among the different MCDM models, the analytic hierarchy process (AHP) is the most extensively applied and well-known for flood hazard mapping. Other notable models in this field include the frequency ratio (FR), Shannon entropy, and weight of evidence. According to Mudashiru *et al*.,[17] the application of empirical models in flood hazard mapping has increased by 35% from 2000 to 2019.[17] The shift from labor-intensive manual flood risk assessment technologies to high-tech digital methods has enhanced risk assessment accuracy.[18] The advent of different modern software, like Geographic Information System (GIS), in the 21st century, has increased the application of modeling approaches in flood research, drawing considerable attention from flood researchers. Remote sensing applications have enhanced the resolution and utilization of models in flood risk assessment and susceptibility mapping. The integration of remote sensing data with GIS, combined with various hydrologic and hydrodynamic models, has enabled flood hazard, risk, and vulnerability mapping.[19]

2. Study area

The Barak River basin of India is the focus of the present research (Figure 1). The Barak River, originating from Manipur, flows through Assam and further downstream through Bangladesh, ultimately emptying into the Bay of Bengal. The river basin area spans several states in India, including Meghalaya, Nagaland, Tripura, Manipur, Mizoram, and Assam. After passing through the Cahar district of Assam, the river enters Bangladesh, and in certain places, it demarcates the boundary between India and Bangladesh. Physiographically, the Barak River basin is surrounded by hilly terrains on three sides: (i) the northern side is bordered by the North Cachar

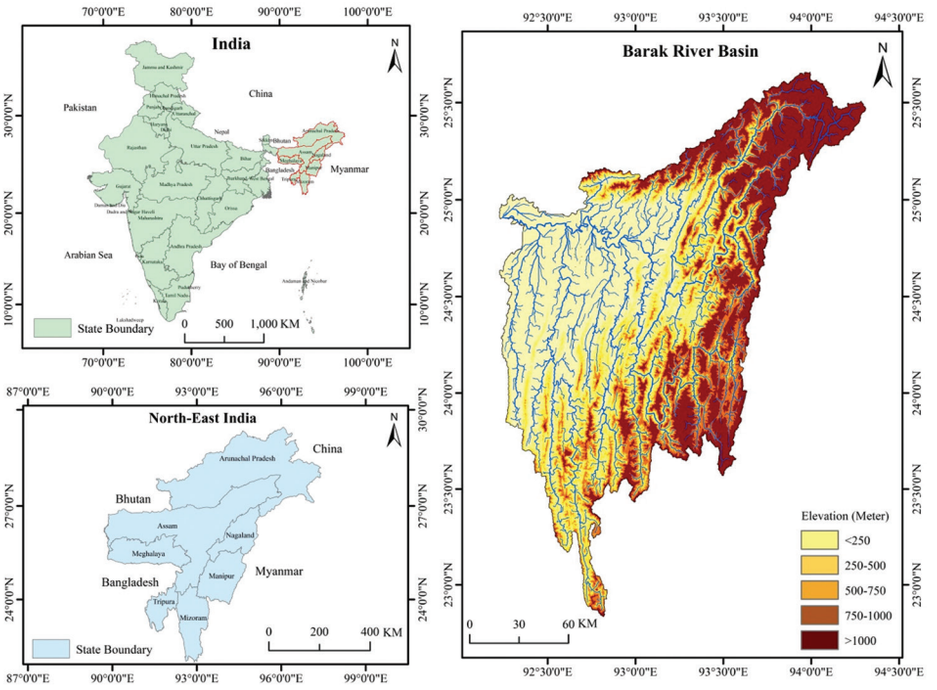

Figure 1. The study area map

Hills, (ii) the north-eastern and eastern sides are defined by the Naga and Barail ranges, and (iii) the southern and south-eastern sides are composed of Mizo hills.

The central, eastern, and Bangladesh parts of the basin are floodplains of the river, which are highly flood-prone. Flooding is a recurring event in the Barak River floodplain; each year during monsoon season, large areas get inundated by river floods, causing significant property and crop damage and disrupting the communication system. Major floods occurred in the study area in 1991, 1994, 1996, 2004, and 2009.[20] Floods in the Barak River basin are frequent and severely impact the Barak Valley of Assam, which comprises three districts: Cachar, Karimganj, and Halikandi, with a total geographical area of 6,922 km^2. Silchar, the second largest city of Assam, is located in the Cachar district along the banks of the Barak River. Barak Valley is one of the most densely populated regions of Assam, with a population of 1,736,617. Cachar is the second-most populated district, while Karimganj and Hailakandi have populations of 1,228,686 and 659,296, respectively. These populations are spread across 2,307 villages and town areas.[21,22]

3. Methodology

Figure 2 shows the methodological flowchart. Eight flood conditioning factors – drainage density, drainage frequency, topographic wetness index (TWI), slope, elevation, distance from the river, distance from the road, and geology – were used for the analysis. Secondary data were utilized to prepare all the model input layers. The training and validation flood points were drawn from the National Remote Sensing Centre generated flood inundation maps of 14th July 2022 flood. The area under the curve (AUC) method validated the generated maps. After the preparation of the input layers, input parameter weights were calculated for both Shannon's entropy and FR models. In the second stage, after delineating flood hazard-susceptible areas, the flood risk of the hazard-susceptible villages was studied. For risk assessment, village boundaries, and associated parameter data were derived using the Census of India 2011. Weights were assigned to four indicators for exposure assessment: village-level elevation, river length, normalized difference vegetation index (NDVI), and normalized difference water index (NDWI) using the AHP method. Similarly, weightages were assigned to six indicators – population density, household density, child population (0 – 6 years), illiteracy rate, marginal workers, and agricultural workers – for assessing the vulnerability of the villages. In the final stage, the risk index of the villages was derived by combining both the exposure and vulnerability indices.

3.1. Shannon's entropy model

Entropy measures each system's instability, abnormality, and unbalanced behavior.[23] The theory

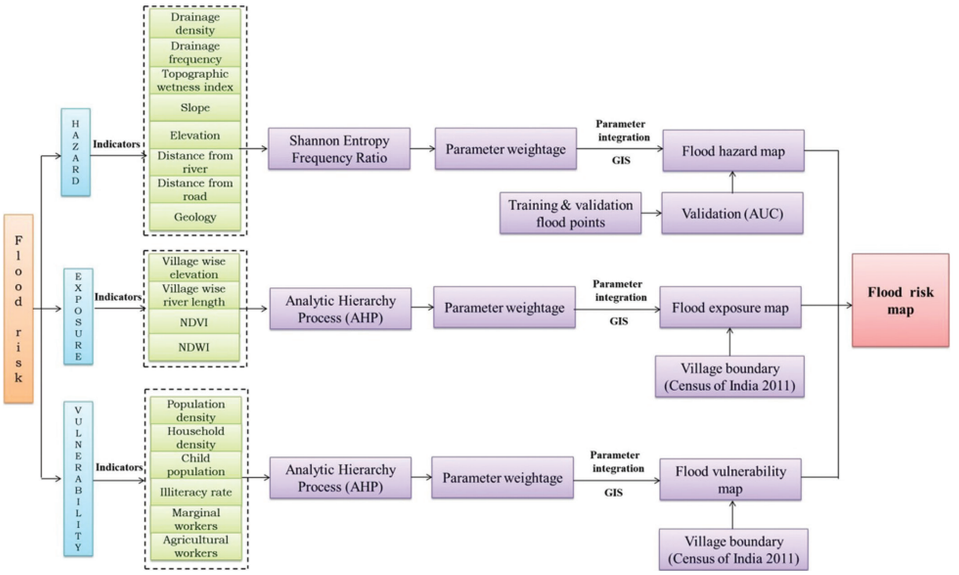

Figure 2. The methodological flowchart

Abbreviations: AUC: Area under the curve; GIS: Geographic Information System; NDVI: Normalized difference vegetation index; NDWI: Normalized difference water index.

was first introduced by Stefan-Boltzmann, with Shannon formalizing the numerical induction in 1948. Shannon later expanded the model into information theory, building upon the Boltzmann theorem.[24] The entropy model is extensively applied for risk and hazard assessments to calculate weighted indices of natural hazards and prioritize influencing factors.[25] The entropy weights of all indicators and the final susceptibility were determined using the following equations. Entropy weights were calculated for all indicators, and subsequent susceptibility zone maps were created using the following procedures and formulas.

(i) Step 1: Normalize the value of each indicator to calculate index weight using Equation I.

$$y_{ij} = \frac{X_{ij}}{\sum_{i=0}^{m} X_{ij}}, 0 \le y_{ij} \le 1 \quad \text{(I)}$$

where, y_{ij} is the specific gravity value for each X_{ij}, and m is the number of evaluation objects. X_{ij} is derived from the FR value, and i represents a class of j flood conditioning factor.

(ii) Step 2: Define entropy for each indicator j using Equation II.

$$e_{j=-k} \sum_{i=1}^{m} y_{ij} \ln y_{ij} \quad \text{(II)}$$

where e_j is the entropy value. The coefficient k is determined by the sample size (number of evaluating objects), m, using Equation III.

$$k = \frac{1}{\ln m} \quad \text{(III)}$$

The information utility value for each indicator h_j is derived from Equation IV.

$$h_j = 1 - e_j \quad \text{(IV)}$$

(iii) Step 3: Calculate the entropy weight of each indicator using Equation V.

$$w_j = \frac{h_j}{\sum_{j=1}^{n} h_j} \quad \text{(V)}$$

where w_j is the weight of the ith indicators, and n is the number of attribute indicators.

(iv) Step 4: Define the flood susceptibility mapping using Equation VI.

$$FSI = \sum_{j=1}^{n} w_j \, Nor\left(F_j\right) \quad \text{(VI)}$$

where FSI is the degree of flood susceptibility index, w_j stands for the weight of each indicator and $Nor\left(F_j\right)$ is the normalized rate for each flood indicator.

3.2. FR

The FR model is a bivariate statistical method commonly used in hazard and disaster susceptibility analysis. Its simplicity and effectiveness in predicting flood likelihood make it a popular choice for estimating hazard likelihood. The model calculates the likelihood of future flood occurrence by analyzing the distribution of past flood events across various factors.[26] This model suggests that the importance of a specific factor in predicting flood occurrence is directly corresponding to the ratio of its class within the controlling factor. The FSI for a pixel is determined by summing the flood frequencies of all factors associated with that pixel.[27] The model estimates pixel-wise flood potential by pixel-wise FR of all factors, which is calculated as an equation.

$$FR_{ij} = \frac{Lc}{Lt} / \frac{Af}{At} \quad \text{(VII)}$$

The FR of the factor classes has been calculated using Equation VII, where *Lc* indicates the training flood location in i^{th} class of flood conditioning factor *j*, *Lt* is the total number of training flood points, *Af* is the area or pixel number in the i^{th} class of *j* flood conditioning factor, and *At* is the total pixel count or area of the *j* factor.

3.3. Receiver operating characteristics curve

The AUC is used to validate or examine the capability of a model to predict the probability of occurrence of hazards and disasters. The receiver operating characteristics curve (ROC) is the tradeoff between false positive and accurate positive rates along the X and Y axes.[28] Plotting the sensitivity, quantification of the successful and non-successful events, and 1-specificity on the abscissa and ordinates are the key aspects of it.[29,30] The value of the AUC curve varies between 0.5 and 1.0; a value between 0.9 and 1.0 indicates excellent success or prediction rate, 0.8 – 0.9 indicates very good, 0.7 – 0.8 indicates good, 0.6 – 0.7 indicates moderate, and <0.6 indicates weak prediction rate of the model.[26,31] The AUC equation is presented in Equation VIII,

$$AUC = \frac{\Sigma TP + \Sigma TN}{P + N} \quad \text{(VIII)}$$

where *TP* or true positive is the flood pixels and *TN* or true negative is the non-flood pixels. *P* is the flood point sum, and *N* is the number of non-flood points.

4. Results and discussion

4.1. Flood hazard conditioning factors

4.1.1. Drainage density

Drainage density refers to the length of the channels in a drainage basin divided by the basin's total area.[32] It is considered one of the most important parameters of fluvial landscape evolution under the influence of rivers. Consequently, there is a positive correlation between drainage density and flooding. As a result, the likelihood of flooding increases with higher stream network density.[33] As shown in Figure 3, the drainage density of the study area has been categorized into five classes based on its spatial pattern, which reveals that all the drainage density classes have almost similar pixel counts. A positive correlation was noticed between the drainage density classes and their FRs. The very high drainage density class had the highest FR (47.93%) and vice versa. The floodplains of the Barak River basin have high (0.3 – 0.4) to very high (>0.4) drainage density, which defines its higher susceptibility to flooding.

4.1.2. Elevation

Elevation is a primary determinant of flood vulnerability. Studies have shown that elevation is the most influential variable in flood occurrence, with lower elevations correlating to a higher likelihood of inundation.[23] The analysis shows a considerable variation in elevation from mountains to floodplains of the Barak River basin. Figure 3 represents the elevation map of the study area, where the entire Barak River basin is classified into five elevation zones. The highest proportion (33.04%) of the study area topography has elevations <250 m, followed by very high (>1.000), which represents 21.82% of the study area. The very low elevated areas of the Barak River basin have 100% FRs, which indicates the flood occurrence in the study area and is bounded in the low elevated regions.

4.1.3. Slope

The slope is a measure of how steeply a line or surface inclines. It is calculated as the change in height relative to the horizontal distance and expressed as a percentage or angle. It significantly influences surface runoff and water infiltration into the ground, which makes it a crucial factor in studying and predicting flood occurrence.[27] Figure 3 shows the slope map of the Barak River basin, which has been categorized into five classes. The hilly surrounding regions have high (20 – 25°) to very high (>25°) slopes, and the

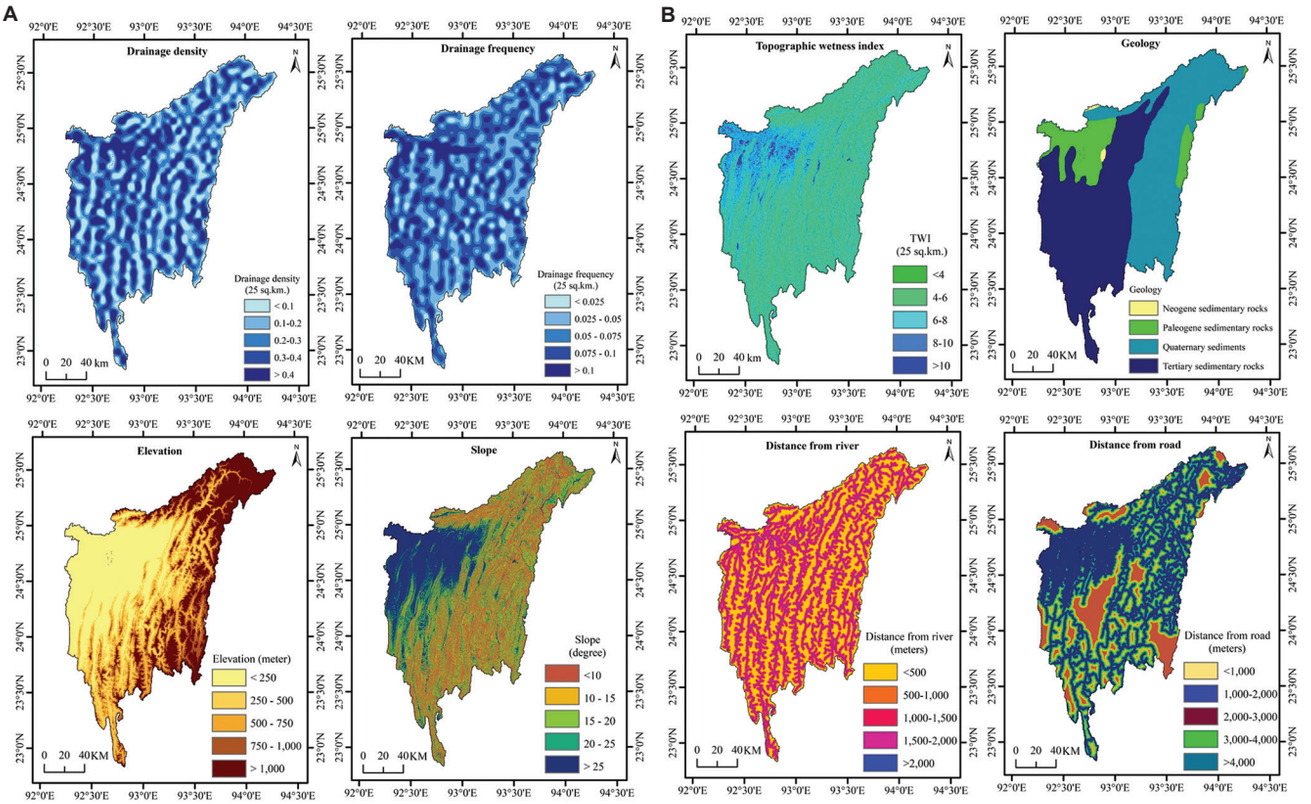

Figure 3. (A and B) Flood conditioning parameters

floodplains have a slope <10°. The calculated FR of different slope classes reveals that pixels with very low (<10°) slope values are highly susceptible to flood inundation.

4.1.4. Drainage frequency

Drainage frequency is the number of stream segments per unit area.[32] Various factors significantly influence stream frequency, including rock type, terrain ruggedness, slope steepness, rainfall patterns, subsurface material properties, vegetation cover, and drainage density. A higher stream frequency is generally associated with a denser drainage network. This indicates a landscape actively shaped by erosion and fluvial processes. Consequently, areas with high stream frequencies often exhibit a greater risk of flooding due to increased sediment load and reduced infiltration. However, these regions may also possess higher groundwater potential due to increased percolation.[34] The study area has been classified into five drainage frequency zones. FR analysis indicates a positive relationship between drainage frequency and flood susceptibility. Regions with high drainage frequencies exhibit a higher probability of flood occurrence.

4.1.5. TWI

The TWI is an effective parameter for measuring long-term moisture availability in topography. It quantifies the effect of local topography on runoff and overland flow generation.[35] The area's TWI provides insights into two key factors: terrain shape and hydrological conditions. This index quantifies the water content of each grid cell within the study area. Essentially, TWI highlights the variations in water saturation across a region.[33] Hence, it effectively contributes to flood occurrence. As shown in the TWI map, the water body surrounding areas and the downstream floodplains have high to very high moisture saturation. The class-wise FR is higher in areas with moisture-saturated TWI zones. As the TWI decreases, the class FR also decreases.

4.1.6. Geology

The geological characteristics of a region play a crucial role in determining flood hazards. Factors such as the rocks' infiltration and permeability are closely related and influence flood potential. Geology is also essential for reconstructing past flood occurrences.[4] The study area geology map has been extracted from the United States Geological Survey geology map of South Asia. The study area consists of four

Table 1. Assigning weights to the parameters and subclasses using the frequency ratio model

Class name/description	Pixel count	Percentage (%)	Number of floods	% of the number of floods	Frequency ratio	Rf	Rf (%)	Min (Rf)	Max (Rf)	Max–min (Rf)	(Max-min) Min Rf	Pr
Drainage density												
<0.1	5,312,800	15.75	5	4.13	0.26	0.05	5					
0.1 – 0.2	6,752,868	20.02	5	4.13	0.21	0.04	4					
0.2 – 0.3	7,788,913	23.09	22	18.18	0.79	0.16	16					
0.3 – 0.4	6,950,116	20.60	31	25.62	1.24	0.26	26					
>0.4	6,926,391	20.53	58	47.93	2.33	0.48	48					
Sum					4.83			0.04	0.48	0.44	0.19	2.35
Drainage frequency												
<0.025	1,803,030	5.35	1	0.83	0.15	0.03	3					
0.025 – 0.05	7,767,919	23.03	13	10.74	0.47	0.09	9					
0.05 – 0.075	9,156,685	27.15	24	19.83	0.73	0.14	14					
0.075 – 0.1	9,714,041	28.80	28	23.14	0.80	0.16	16					
>0.1	5,289,412	15.68	55	45.45	2.90	0.57	57					
Sum					5.05			0.03	0.57	0.54	0.19	2.86
Topographic wetness index												
<4.0	1,405,762	4.17	0	0	0	0	0					
4.0 – 6.0	17,854,614	52.92	8	6.61	0.12	0.02	2					
6.0 – 8.0	8,712,863	25.83	52	42.98	1.66	0.22	22					
8.0 – 10.0	3,314,004	9.82	34	28.10	2.86	0.37	37					
>10.0	2,449,204	7.26	27	22.31	3.07	0.40	40					
Sum					7.72			0	0.40	0.40	0.19	2.09
Slope												
<10	9,296,726	27.56	119	98.35	3.57	0.97	97					
10 – 15	4,477,825	13.27	1	0.83	0.06	0.02	2					
15 – 20	5,027,928	14.90	1	0.83	0.06	0.02	2					
20 – 25	5,033,950	14.92	0	0	0.00	0.00	0					
>25	9,900,018	29.35	0	0	0.00	0.00	0					
Sum					3.69			0.00	0.97	0.97	0.19	5.10

(Cont'd...)

doi: 10.36922/AJWEP025040019

Table 1. ***(Continued)***

Class name/description	Pixel count	Percentage (%)	Number of floods	% of the number of floods	Frequency ratio	Rf	Rf (%)	Min (Rf)	Max (Rf)	Max–min (Rf)	(Max-min) Min Rf	Pr
Geology												
Neogene sedimentary rock	16,390,344	48.59	47	38.84	0.80	0.04	4					
Paleogene sedimentary rock	13,106,647	38.86	0	0.00	0.00	0.00	0					
Quaternary sediments	4,126,165	12.23	69	57.02	4.66	0.25	25					
Tertiary sedimentary rock	107,931	0.32	5	4.13	12.91	0.70	70					
Sum					18.38			0.00	0.70	0.70	0.19	3.70
Distance from road												
<1000	17,186,661	50.95	119	98.35	1.93	0.96	96					
1000 – 2000	6,918,887	20.51	2	1.65	0.08	0.04	4					
2000 – 3000	3,760,359	11.15	0	0	0	0	0					
3000 – 4000	2,113,104	6.26	0	0	0	0	0					
>4000	3,752,077	11.12	0	0	0	0	0					
Sum					2.01			0	0.96	0.96	0.19	5.05
Distance from river												
<500	1,827,179	5.42	10	8.26	1.53	0.26	26					
500 – 1000	6,529,764	19.36	29	23.97	1.24	0.21	21					
1000 – 1500	7,023,579	20.82	38	31.40	1.51	0.26	26					
1500 – 2000	6,069,805	17.99	25	20.66	1.15	0.20	20					
>2000	12,280,761	36.41	19	15.70	0.43	0.07	7					
Sum					5.85			0.07	0.26	0.19	0.19	0.98
Elevation												
<250	11,146,025	33.04	121	100	3.03	1	100					
250 – 500	5,200,503	15.42	0	0	0	0	0					
500 – 750	5,330,397	15.80	0	0	0	0	0					
750 – 1000	4,699,604	13.93	0	0	0	0	0					
>1000	7,359,918	21.82	0	0	0	0	0					
Sum					3.03			0	1	1	0.19	5.26

Abbreviations: Pr: Final parameter weightage; Rf: Frequency ratio.

doi: 10.36922/AJWEP025040019

major geological formations: (i) Neogene sedimentary rock, (ii) Paleogene sedimentary rock, (iii) quaternary sediments, and (iv) tertiary sedimentary rock. Notably, 48.59% and 38.86% of the Barak River basin have Neogene and Paleogene sedimentary rock formations, respectively. Neogene sedimentary rock is found along the middle, eastern, and southern parts, and the quaternary sediments are found throughout the floodplains of the Barak River. The FR distribution (Tables 1 and 2) reveals that a significant proportion of past flood events have occurred in the regions composed of Neogene sedimentary rocks and quaternary sediments.

4.1.7. Distance from road

The distance from a road is a significant parameter in assessing flood risk. Due to their impervious nature, roads reduce the absorption of rainwater into the ground, contributing to increased runoff and potential flooding.[27] In addition, they may act like artificial barriers in surface runoff flow. Road network defines the connectivity and accessibility of any particular area. Occurrence of any hazard and disaster damages road connectivity, which makes any area inaccessible during the disastrous events. This makes the distance from the road an essential

Table 2. Assigning weights to the parameters and subclasses using Shannon's entropy model

Class name/description	Pixel count	Percentage (%)	Number of floods	% of the number of floods	Frequency ratio	SE			
						Pij	*Ej*	*h=1-e$_j$*	*Wj*
Drainage density								0.199	0.05
<0.1	5,312,800	15.75	5	4.13	0.26	0.05	−0.07		
0.1 – 0.2	6,752,868	20.02	5	4.13	0.21	0.04	−0.06		
0.2 – 0.3	7,788,913	23.09	22	18.18	0.79	0.16	−0.13		
0.3 – 0.4	6,950,116	20.60	31	25.62	1.24	0.26	−0.15		
>0.4	6,926,391	20.53	58	47.93	2.33	0.48	−0.15		
Sum					4.83	1.00	0.801		
Drainage frequency								0.244	0.06
<0.025	1,803,030	5.35	1	0.83	0.15	0.03	−0.05		
0.025 – 0.05	7,767,919	23.03	13	10.74	0.47	0.09	−0.1		
0.05 – 0.075	9,156,685	27.15	24	19.83	0.73	0.14	−0.12		
0.075 – 0.1	9,714,041	28.80	28	23.14	0.80	0.16	−0.13		
>0.1	5,289,412	15.68	55	45.45	2.90	0.57	−0.14		
Sum					5.05	1.00	0.756		
Topographic wetness index								0.297	0.07
<4.0	1,405,762	4.17	0	0.00	0.00	0	0		
4.0 – 6.0	17,854,614	52.92	8	6.61	0.12	0.02	−0.03		
6.0 – 8.0	8,712,863	25.83	52	42.98	1.66	0.22	−0.14		
8.0 – 10.0	3,314,004	9.82	34	28.10	2.86	0.37	−0.16		
>10.0	2,449,204	7.26	27	22.31	3.07	0.40	−0.16		
Sum					7.72	1	0.703		
Slope								0.898	0.22
<10	9,296,726	27.56	119	98.35	3.57	0.97	−0.01		
10_15	4,477,825	13.27	1	0.83	0.06	0.02	−0.03		
15 – 20	5,027,928	14.90	1	0.83	0.06	0.02	−0.03		
20 – 25	5,033,950	14.92	0	0.00	0.00	0.00	0		
>25	9,900,018	29.35	0	0.00	0.00	0.00	0		
Sum					3.69	1.00	0.102		

(Cont'd...)

Table 2. ***(Continued)***

Class name/description	Pixel count	Percentage (%)	Number of floods	% of the number of floods	Frequency ratio	SE			
						Pij	*Ej*	*h=1-e$_j$*	*Wj*
Geology								0.472	0.12
Neogene sedimentary rock	16,390,344	48.59	47	38.84	0.80	0.04	−0.06		
Paleogene sedimentary rock	13,106,647	38.86	0	0.00	0.00	0.00	0		
Quaternary sediments	4,126,165	12.23	69	57.02	4.66	0.25	−0.15		
Tertiary sedimentary rock	107,931	0.32	5	4.13	12.91	0.70	−0.11		
Sum					18.38	1.00	0.528		
Distance from road								0.896	0.22
<1000	17,186,661	50.95	119	98.35	1.93	0.96	−0.02		
1000 – 2000	6,918,887	20.51	2	1.65	0.08	0.04	−0.06		
2000 – 3000	3,760,359	11.15	0	0.00	0.00	0	0		
3000 – 4000	2,113,104	6.26	0	0.00	0.00	0	0		
>4000	3,752,077	11.12	0	0.00	0.00	0	0		
Sum					2.01	1.00	0.104		
Distance from river								0.043	0.01
<500	1,827,179	5.42	10	8.26	1.53	0.26	−0.15		
500 – 1000	6,529,764	19.36	29	23.97	1.24	0.21	−0.14		
1000 – 1500	7,023,579	20.82	38	31.40	1.51	0.26	−0.15		
1500 – 2000	6,069,805	17.99	25	20.66	1.15	0.20	−0.14		
>2000	12,280,761	36.41	19	15.70	0.43	0.07	−0.08		
Sum					5.85	1.00	0.957		
Elevation								1	0.25
<250	11,146,025	33.04	121	100.00	3.03	1	0		
250 – 500	5,200,503	15.42	0	0.00	0.00	0	0		
500 – 750	5,330,397	15.80	0	0.00	0.00	0	0		
750 – 1000	4,699,604	13.93	0	0.00	0.00	0	0		
>1000	7,359,918	21.82	0	0.00	0.00	0	0		
Sum					3.03	1	0		

Abbreviation: SE: Shannon's entropy.

parameter of flood damage. The road distance layer of the study has been delineated on both sides of roads using the Euclidean distance method in GIS.

4.1.8. Distance from river

The distance from a river is a key factor in determining the severity and reach of a flood. Areas closer to the river are generally at greater risk of more intense flooding and a wider spread of floodwater.[27] According to Wang *et al*.,[36] globally, a trend of relocating away from flood-inundated areas was observed in 53% of countries from 2000 to 2018, which ultimately resulted in a reduction in flood exposure, fatalities, and displacement.[36] The Shuttle Radar Topography Mission with a digital elevation model was used for stream extraction. The distance from the river was delineated on both sides of vectorized streams using the Euclidean distance method in GIS.

4.2. Flood hazard analysis and validation

Flood susceptibility maps were created using GIS (Figure 4). These maps were based on the relative importance of different flood conditioning factors, as determined by FR and Shannon entropy analyses. An FSI was calculated by combining information from all identified flood-inducing factors. Higher FSI values indicate a greater likelihood of flooding, while lower values suggest a lower risk. To categorize flood risk, the

Table 3. Class-wise area distribution of different flood susceptibility classes

Flood susceptibility	Frequency ratio model	Frequency ratio	Shannon entropy model	Shannon entropy
Very low	9,268.80	33	9,272.72	33
Low	10,338.74	37	10,458.77	38
Moderate	2,968.71	11	2,052.30	7
High	2,292.23	8	1,438.42	5
Very high	2,874.20	10	4,520.47	16
	2,7742.68	100.00	27,742.68	100.00

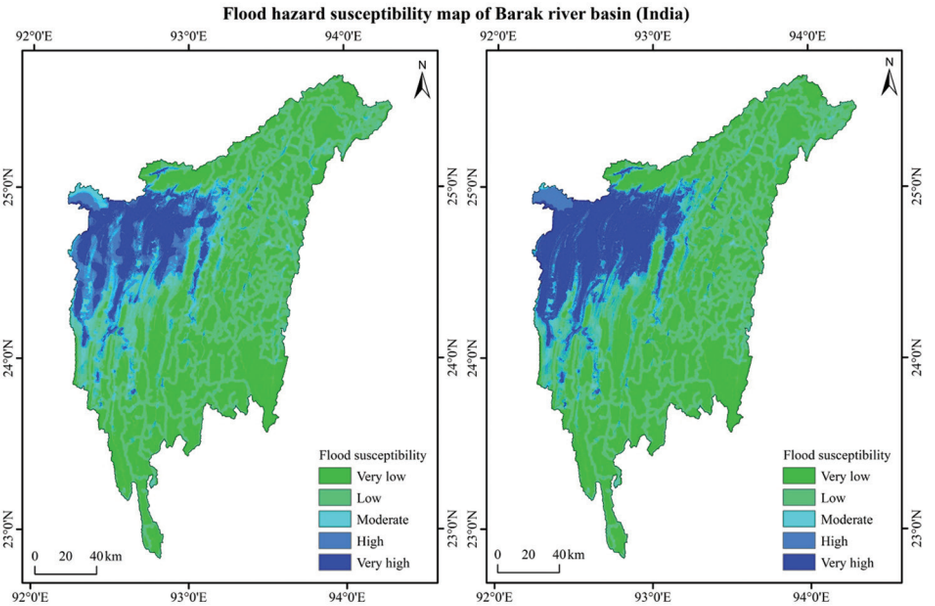

Figure 4. Flood susceptibility maps showing (A) frequency ratio and (B) Shannon's entropy

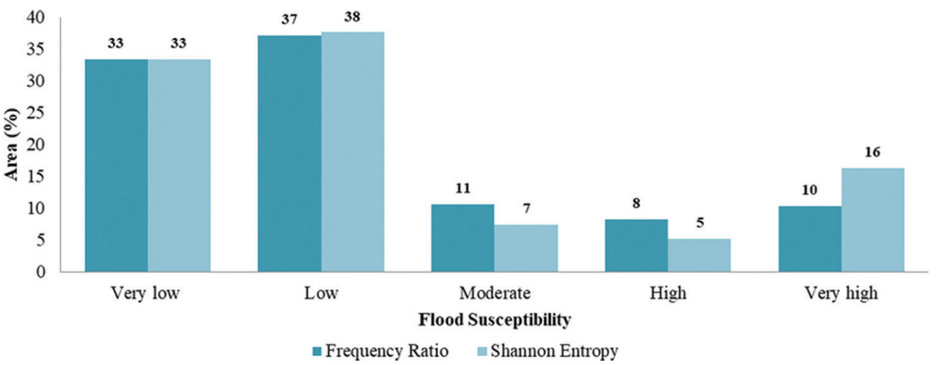

Figure 5. The area distribution of different flood susceptibility classes

study area was classified into five susceptibility zones based on FSI values. According to Table 3 and Figure 5, both the hazard maps indicate that around 70% of study areas have low to very low susceptibility to floods, around 10% are moderately susceptible, and around 20% are highly and very highly flood-susceptible.

The Barak Valley in Assam, a region of significant concern, is highly vulnerable to flooding. The lower floodplain of the Barak River basin, covering a total of 4,513.42 km^2, is at high risk. This area, which includes the districts of Cachar, Karimganj, and Hailakandi, is particularly susceptible to floods. According to

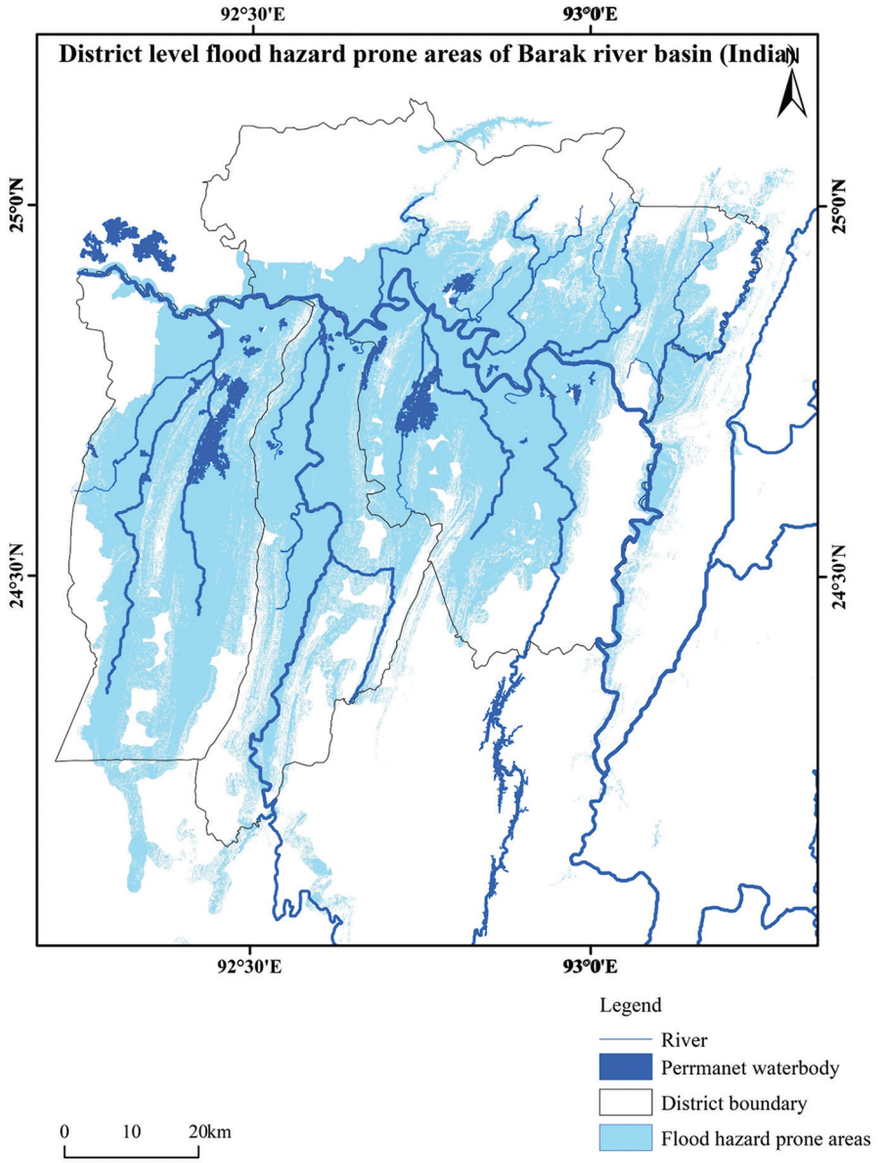

Figure 6. Flood-prone areas of the lower Barak River basin

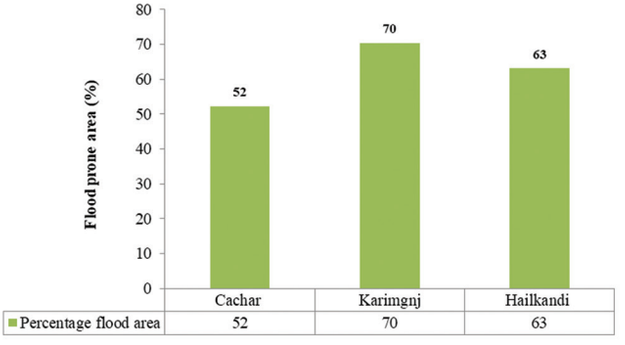

Figure 7. District-wise flood susceptibility area distribution

the generated flood maps (Figure 6), the districts of Cachar, Karimganj, and Hailakandi have 1,973.37, 1,273.27, and 840.88 km^2, respectively, classified as very highly flood-prone. In terms of percentage (Figure 7), Karimganj is the most vulnerable, with 70% of its area affected, followed by Hailakandi at 63% and Cachar at 52%.

A validation process is essential for assessing the accuracy of the generated flood hazard susceptibility maps. The present study utilized the AUC method to assess the accuracy of the maps. A total of 200 flood points were sourced from IRS-published maps of

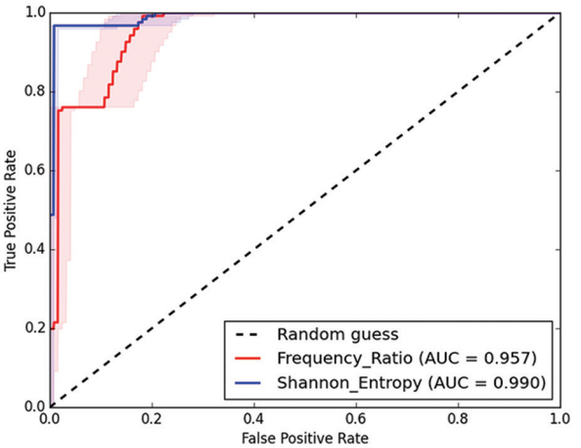

Figure 8. The area under the curve of generated flood hazard maps

different flood events. Of these, 80 points served as training points to correlate with conditioning factors, and 120 points were utilized for validation. As shown in Figure 8, the AUC values for the FR and Shannon's entropy models were calculated as 0.957 and 0.99, respectively, indicating acceptable performance for both in predicting flood hazard susceptibility. However, the entropy model demonstrated superior accuracy to the FR model, as evidenced by its higher AUC value.

4.3. Flood vulnerability assessment

Vulnerability refers to how likely people are to be harmed by natural disasters, accidents, or economic downturns. This harm can be physical, social, or economic.[37] It encompasses the potential for loss of life, property damage, and disruption of livelihoods. The flood vulnerability index provides a simplified measure of harm susceptibility through physical, social, and economic factors. It helps to identify the potential flood-vulnerable areas and can direct future mitigation and adaptation strategies.[38] Vulnerability can be classified as social vulnerability, economic vulnerability, physical vulnerability, and environmental vulnerability. Physical vulnerability includes infrastructure and agricultural activity; social vulnerability includes children, women, old, disabled people, refugees, and livestock; and economic vulnerability is related to economic losses related to hazards and disasters. The scale of flood vulnerability and its potential to turn into a disaster is determined by the value of the receptors or the exposed materials that may be affected by flooding events. This possibility of greater flood damage and losses is often exacerbated by illegal encroachment or occupation of river floodplains.[39] Flood vulnerability of certain regions is a function of exposure to flood susceptibility, adaptive capacity, and elements at risk.[40,41] In the present context, six variables – population density, household density, child population, illiteracy rate, marginal worker, and agricultural worker – were considered at the village level based on the 2011 Census of India. Weights were assigned depending on the level of significance (Table 4). The spatial distribution of vulnerability indicators is represented in Figure 9. The highest weights were assigned to the villages with high household density, high population density, high illiteracy rate, and a high number of marginal and agricultural workers who are directly affected by flooding events. The derived vulnerability map (Figure 10) inferred that 461 villages were highly vulnerable, whereas 485 villages were very highly vulnerable. These villages represent a socio-economically disadvantaged status with a high population, household density, high child population, high number of marginal workers, and illiteracy rate. In contrast, 330 villages were moderately vulnerable, and 310 villages had very low vulnerability, whereas 308 villages had low vulnerability, which depicts improved prevailing socio-economic status compared to previous villages.

4.4. Flood exposure assessment

Exposure is the potentiality of loss of life, resources, and commodities due to external hazardous or disastrous events.[37] The exposure index reflects the places that may be adversely affected and the factors in the environment that will affect floods.[42] In the present study, four variables (Figure 11) – village-river length, village-level elevation, NDVI, and NDWI – were considered for exposure assessment at the village level and assigned appropriate weights. The highest weightages (Table 5) were assigned to the villages with low elevation and villages with high drainage length, high NDWI, and low NDVI, as they are highly exposed to flooding. Flood exposure (Figure 12) in the study area has been scaled into five classes (very high, high, moderate, low, and very low). It is inferred from the exposure map that 530 and 283 villages of the study area have very low and low exposure, respectively; 179 villages are moderately exposed, while 561 and 340 villages are highly and very highly exposed to floods, respectively. These highly exposed villages are situated in the lowest elevated river valleys within the study area.

Table 4. The significant weightage of the vulnerability indicators

Parameters	Normalized AHP weightage (%)	Sub-classes	Functional relation	Rank
Population density	32.35	<200	Direct	1
		200 – 400		2
		400 – 600		3
		600 – 800		4
		>800		5
Household density	24.31	<50	Direct	1
		50 – 100		2
		100 – 150		3
		150 – 200		4
		>200		5
Population (0 – 6)	17.5	<100	Direct	1
		100 – 200		2
		200 – 300		3
		300 – 400		4
		>400		5
Illiteracy rate	12	<15	Direct	1
		15 – 25		2
		25 – 35		3
		35 – 45		4
		>45		5
Agricultural worker	8.12	<50	Direct	1
		50 – 100		2
		100 – 150		3
		150 – 200		4
		>200		5
Marginal worker	5.72	<40	Direct	1
		40 – 80		2
		80 – 120		3
		120 – 160		4
		>160		5

Abbreviation: AHP: Analytic hierarchy process.

4.5. Flood risk assessment

Disaster risk has been defined as the probability of disaster occurrence and its projected future damage or how badly it can affect any society. Disaster risk assessment is an essential step to being prepared and ready to act before a disaster strikes.[43] The term flood risk on different occasions has been elaborated similarly, emphasizing various elements by different scientists,[44] as shown in Equations IX to XIII.

$$\text{Risk} = \text{Hazard} \times \text{Vulnerability} \quad \text{(IX)}$$

$$\text{Risk} = \text{Impact of hazard} \times \text{Elements at risk} \times \text{Vulnerability of elements at risk} \quad \text{(X)}$$

$$\text{Risk} = \text{Hazard} \times \text{Vulnerability} \times \text{Value (of the threatened area)/preparedness} \quad \text{(XI)}$$

$$\text{Risk} = \text{Probability} \times \text{Consequences} \quad \text{(XII)}$$

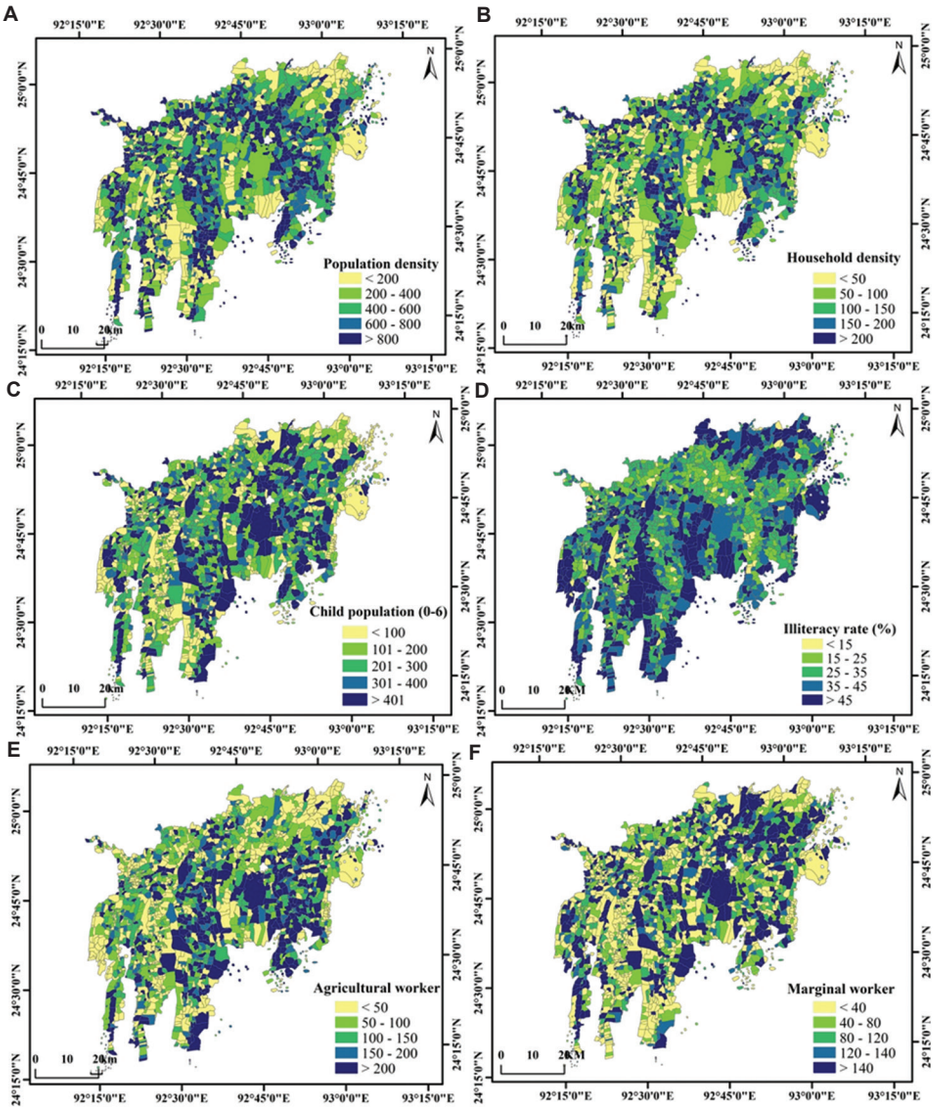

Figure 9. The vulnerability indicators showing the (A) population density, (B) household density, (C) child population, (D) illiteracy rate, (E) agricultural worker, and (F) marginal worker of the Barak River floodplain

$$\text{Risk} = \text{Hazard} \times \text{Consequences} \quad \text{(XIII)}$$

The present study combines the exposure and vulnerability index to derive the flood risk of Barak River floodplain villages. The risk map (Figure 13) is classified into five categories (very high, high, moderate, low, and very low) based on the risk level. It is inferred that among the total number of villages (Figure 14), 388 and 476 Barak River floodplain villages are at very high and high flood risk, 369 villages are at moderate risk, and 343 and 318 villages are at low and very low risk, respectively. It has been observed that 45.61% of severely flood risk-prone villages are located along the main tributary banks of the Barak River, confined with the lowest elevation and high soil moisture saturation. At the same time, 661 least risk-prone villages, which are unaffected by flood events, are located at high elevations relative to the previous villages. As elevation increases toward the surrounding hills, both the elevation and flood risk decrease, contributing to the lower flood vulnerability of these villages.

4.6. Discussion

Floods, a leading global natural disaster, cause substantial damage to life and property. This study

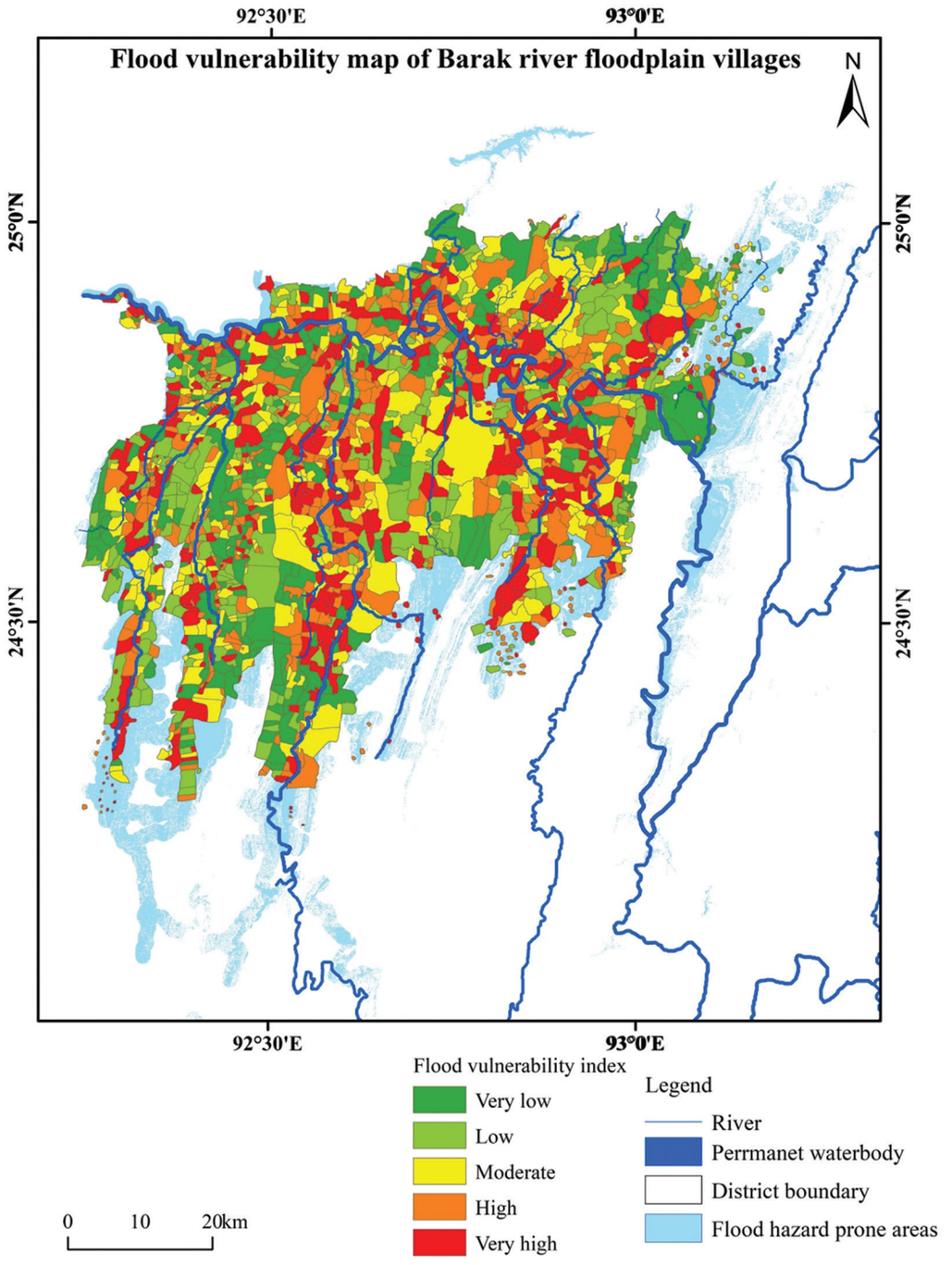

Figure 10. The vulnerability index of Barak River floodplain villages

delineates the flood-susceptible areas and assesses the risk to villages of the Barak River basin. Barak Valley of Assam is densely populated and is highly prone to flooding, which makes it essential to identify areas at risk for effective disaster management strategies. Flood modeling and susceptibility mapping are crucial for assessing vulnerability and developing mitigation plans. Factors, including topography, geology, hydrology, and landforms, contribute to flood occurrence within a river basin. To delineate the flood hazard-prone areas, several factors, such as drainage density, drainage frequency, TWI, slope, elevation, distance from rivers, distance from roads, and geology, were analyzed. The findings of the study indicate that areas below 250 m in elevation and slopes <10° are at high flood risk. In addition, regions with dense drainage networks, frequent

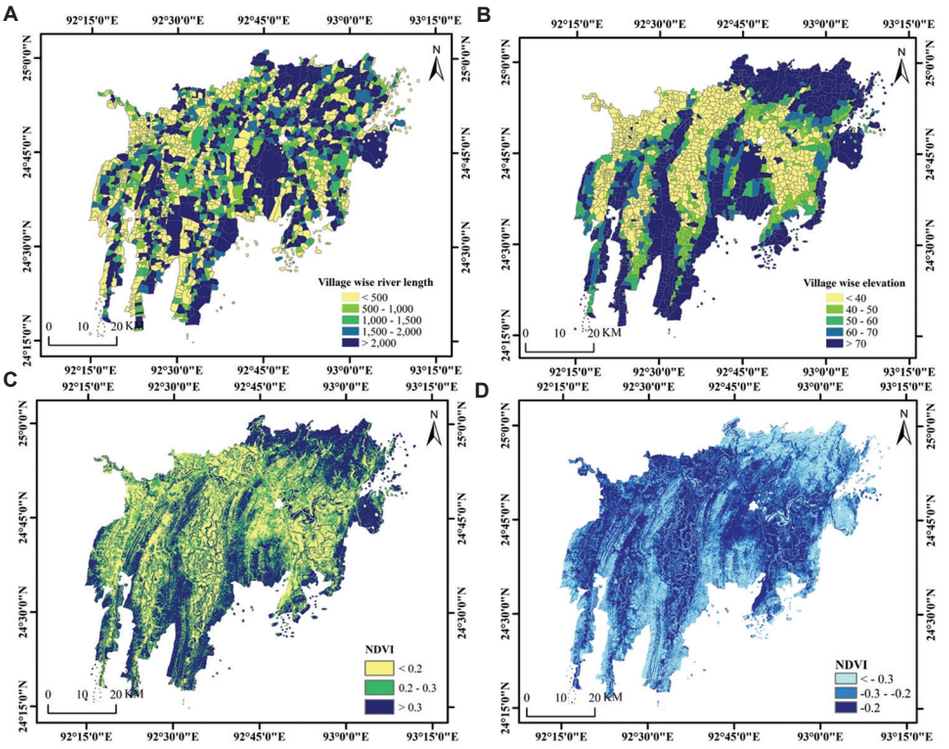

Figure 11. The exposure indicators showing the (A) village river length, (B) village elevation, (C) normalized difference vegetation index, and (D) normalized difference water index

Table 5. The significant weights of the exposure indicators

Parameters	Normalized AHP weightage (%)	Sub-classes	Functional relation	Rank
Village elevation	44.22	<40	Direct	1
		40 – 50		2
		50 – 60		3
		60 – 70		4
		>70		5
Village-wise river length	23.68	<500	Inverse	5
		500 – 1000		4
		1000 – 1500		3
		1500 – 2000		2
		>2000		1
NDWI	17.34	<−0.3	Inverse	3
		−0.3 – −0.2		2
		>−0.2		1
NDVI	13.76	<0.2	Direct	1
		0.2 – 0.3		2
		>0.3		3

Abbreviation: AHP: Analytic hierarchy process; NDVI: Normalized difference vegetation index; NDWI: Normalized difference water index.

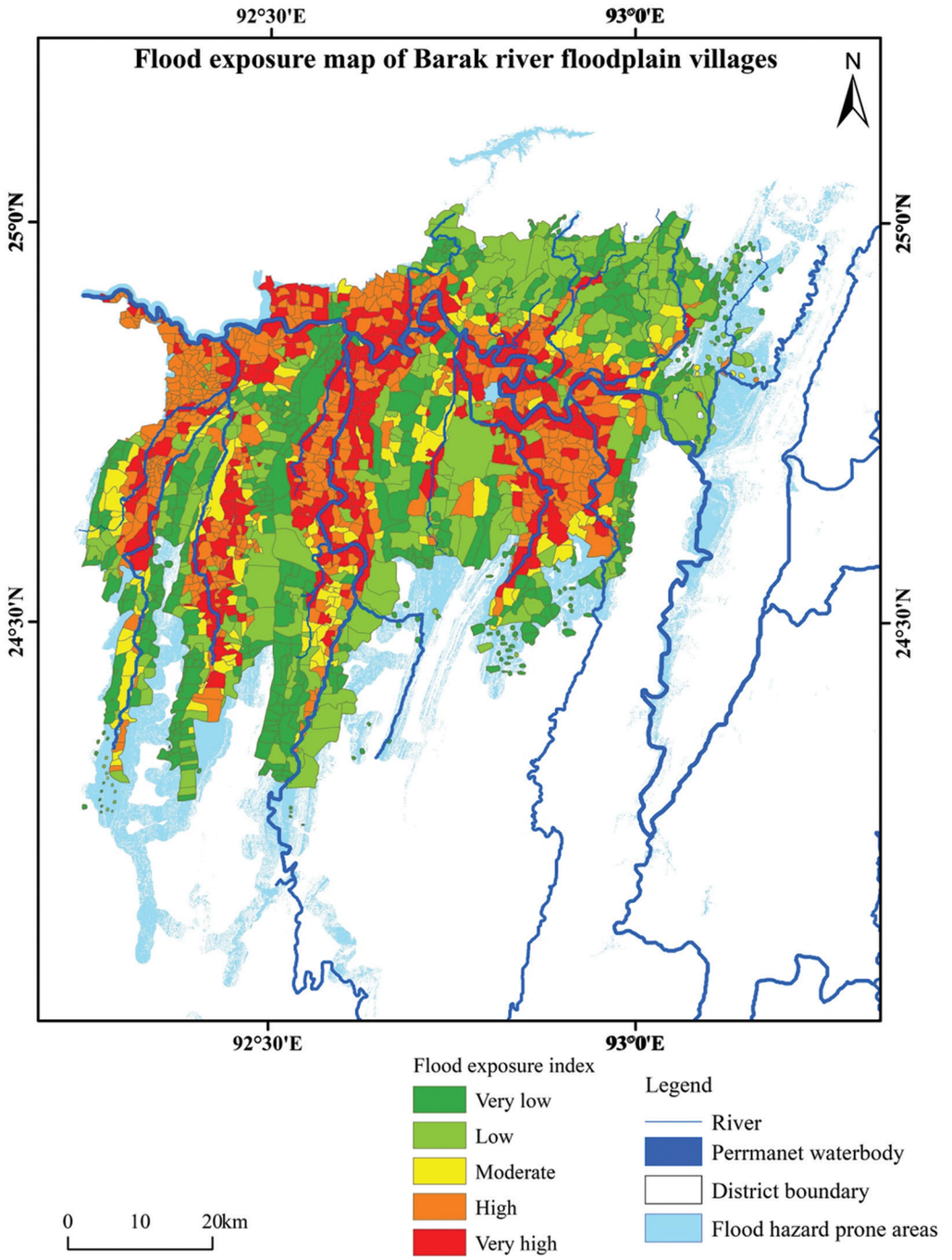

Figure 12. The exposure index of Barak River floodplain villages

watercourses, and proximity to rivers or roads are more likely to experience flooding.

After investigating all the factors, it was found that most of the very highly susceptible areas are concentrated in the eastern and central floodplain of the river. It can be attributed to prevailing factors, such as low elevation, flat plain topography, high topographic and soil moisture content, low slope, and nearby river locations. It makes the area highly flood-susceptible compared to other parts of the study area. According to the FR and entropy model, 18.62 and 21.48% of the basin area have high and very high flood susceptibility, respectively, concentrated in the Barak Valley of Assam (Barak River floodplain). Among the districts, Cachar district has a 1973.37 km² area susceptible to floods, which is the highest among the districts. Karimganj

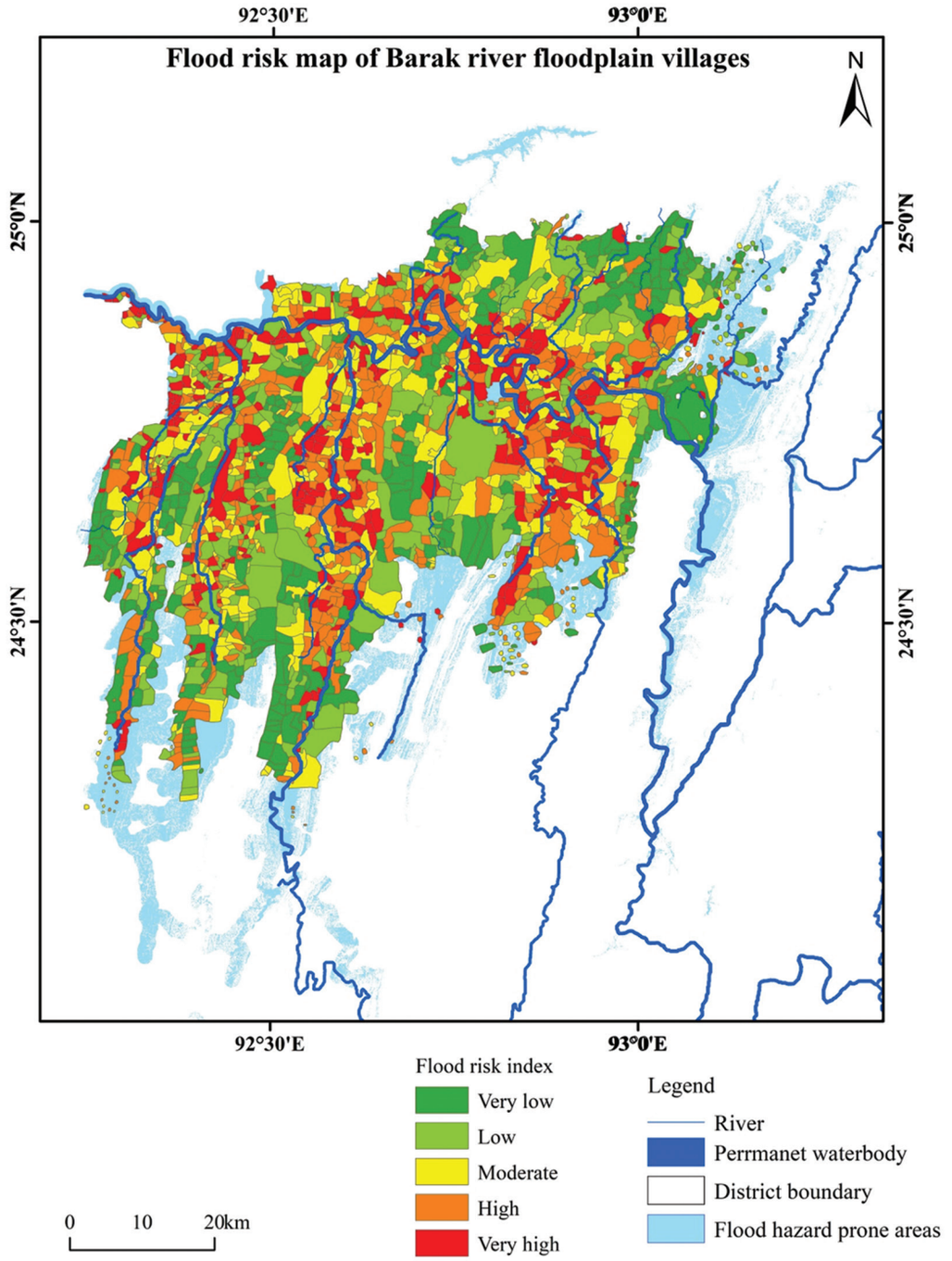

Figure 13. The risk index of Barak River floodplain villages

district, on the other hand, has approximately 70% of its area classified as highly susceptible to floods.

Further study has been carried out to assess the risk of hazard-prone villages and towns. Before risk assessment was conducted, flood vulnerability and flood exposure of the villages were studied. Results of the study revealed that 47.62% of villages are extremely exposed to floods, and these villages are located along the lowest elevated corridors and river banks. Notably, 49.95% of the villages are vulnerable to floods, and these villages are characterized by a socio-economically disadvantaged status. Furthermore, 45.62% of villages are severely prone to flooding, combining both exposure and vulnerability factors. Figure 15 shows the field pictures of Barak Valley flood-affected areas, and Table 6 shows flood damages that occurred at different

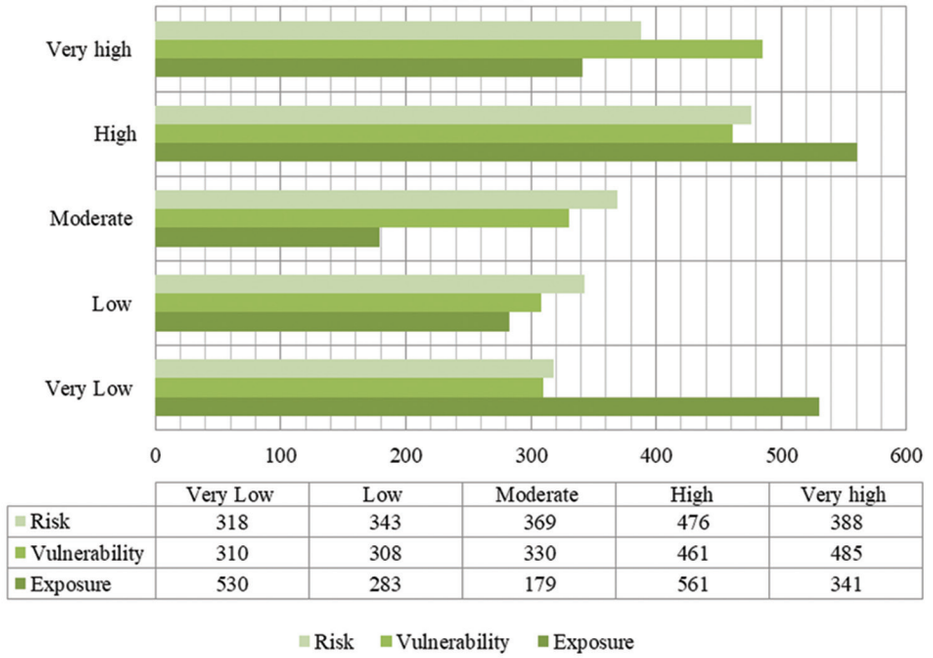

Figure 14. The number of villages with flood exposure, vulnerability, and risk

Figure 15. Field photos of the Barak Valley flood. Image taken by the authors.

times in Barak Valley districts. The data were sourced from the Assam Flood Memorandum 2015 – 2023. The 2022 destructive Assam flood caused great damage in the study area, where 1741 villages and almost 2 million people were affected by the 2022 Barak River flood. In total, 12,809 hectares of agricultural land were inundated, resulting in 56 human fatalities, over 100,000 damaged homes, and additional losses. This was followed by the 2018 flood, which impacted 667 villages, inundated 8,118.62 hectares of agricultural

Table 6. Flood damages in Barak River floodplain districts

District	Flood damage	2015	2016	2017	2018	2019	2022	2023
Cachar	Villages affected	-	-	-	188	55	826	02
	Population affected	5,458		-	-	19,048	1,434,750	565
	Total agricultural land affected (in Ha.)	13,716	0	1,585	1,016	45	8,618	0
	Human life lost	01	-	-	13	-	45	0
	Livestock Assam	-	-	-	-	-	5,211	0
	House damages	01	147	-	53	-	81,544	0
Karimganj	Villages affected	-	-	-	314	55	729	02
	Population affected	18,800	-	-	-	44,048	308,581	214
	Total agricultural land affected (in Ha.)	10,639	1,202	480	2,489.3	595	774	0
	Human life lost	-	-	02	08	-	08	0
	Livestock Assam	-	-	-	-	-	717	0
	House damages	-	2,562	-	-	-	8,518	0
Hailakandi	Villages affected	-	-	-	235	91	186	-
	Population affected	-	-	-	-	4,860	256,019	-
	Total agricultural land affected (in Ha.)	14,725	0	204	4,613.32	1,165	3,417	0
	Human life lost	-	-	-	02	-	03	0
	Livestock Assam	-	-	-	-	-	39	0
	House damages	-	0	-	407	-	28,364	0

land, caused 23 causalities, and damaged 460 houses. The data highlight that flooding and associated damages occur annually in the study area, making floods in the Barak River floodplain a common destructive disaster event. This underscores the need for better planning and management to reduce flood risks and enhance resilience for local communities.

5. Conclusion

Flood susceptibility modeling is a widely used approach in flood management strategies. Researchers often use statistical methods to create flood risk maps. Two popular statistical models, Shannon's entropy and FR, are known for their accuracy and have been utilized in the present study. This study aimed to produce a detailed flood risk map for the study area using geospatial technology. The goal is to identify high-risk zones and develop strategies to protect these areas from future floods. The present study generated flood susceptibility maps by combining eight conditioning factors and model weights. The FR model identified 29.32% of the study area as flood-prone, with 10.36% classified as very high, 8.26% as high, and 10.7% as moderate risk. Similarly, the entropy model indicated 28.88% of the basin as flood-prone, with 16.29% very high, 5.18% high, and 7.4% moderate risk. Both models consistently highlighted the lower Barak River floodplain as a critical flood-prone area. High AUC values (0.95 and 0.99, respectively) confirm the models' reliability, indicating solid predictive performance. Elevation, slope, road network, and road distance emerged as the region's primary factors influencing flood susceptibility. These findings can inform effective flood management strategies to minimize impacts.

Flood risk analysis of the Barak River floodplain villages shows that 866 villages are severely risk-prone to floods, which represents almost 2 million (1,878,366) population which are highly vulnerable, exposed, and risk-prone to floods. These villages are located along the low elevated banks of the Barak River and its tributaries. They are characterized by a high population, household density, a high number of marginal agricultural workers, and a high child population. For better flood management in these areas, specific planning, like flood forecasting, early warning, and floodplain land use planning, should be emphasized.

Acknowledgments

None.

Funding

This study is supported by the University Grant Commission (UGC), India, under the UGC-JRF fellowship (Student ID: 200510423613).

Conflict of interest

The authors declare that they have no competing interests.

Author contributions

Conceptualization: Shanku Ghosh
Formal analysis: Shanku Ghosh
Investigation: Chakkaravarthi Prakasam
Methodology: Chakkaravarthi Prakasam
Writing – original draft: Shanku Ghosh
Writing – review & editing: Chakkaravarthi Prakasam

Availability of data

The study was conducted mainly using secondary data, all of which are publicly available.

References

1. Glas H, Rocabado I, Huysentruyt S, *et al*. Flood risk mapping worldwide: A flexible methodology and toolbox. *Water*. 2019;11:2371. doi: 10.3390/w11112371
2. Rehman S, Hasan Mohd SU, Rai AK, Rahaman MH, Avtar R, Sajjad H. Integrated approach for spatial flood susceptibility assessment in Bhagirathi sub-basin, India using entropy information theory and geospatial technology. *Risk Anal*. 2022;42:2765-2780. doi: 10.1111/risa.13887
3. Duan Y, Xiong J, Cheng W, *et al*. Assessment and spatiotemporal analysis of global flood vulnerability in 2005-2020. *Int J Disast Risk Reduct*. 2022;80:103201. doi: 10.1016/j.ijdrr.2022.103201
4. Adi Prasojo O, Hurst MD, Williams RD, Naylor LA, Toney J. Slowing down the tidal flood wave is the key to reducing tidal flood risk in estuaries worldwide. In: *European Geosciences Union General Assembly*; 2024. doi: 10.5194/egusphere-egu24-17737
5. Duan Y. *Global Projections of Flood Risk Under Climate Change (No. EGU24-7030)*. Copernicus Meetings; 2024.
6. Antwi-Agyakwa KT, Afenyo MK, Angnuureng DB. Know to predict, forecast to warn: A review of flood risk prediction tools. *Water*. 2023;15(3):427. doi: 10.3390/w15030427
7. Di Baldassarre G, Montanari A, Lins H, Koutsoyiannis D, Brandimarte L, Blöschl G. Flood fatalities in Africa: From diagnosis to mitigation. *Geophys Res Lett*. 2010;37(22):1-5. doi: 10.1029/2010gl045467
8. Gupta L, Dixit J. A GIS-based flood risk mapping of Assam, India, using the MCDA-AHP approach at the regional and administrative level. *Geocarto Int*. 2022;37(26):1-33. doi: 10.1080/10106049.2022.2060329
9. Sarkar D, Mondal P. Flood vulnerability mapping using frequency ratio (FR) model: A case study on Kulik river basin, Indo-Bangladesh Barind region. *Appl Water Sci*. 2019;10(1):17. doi: 10.1007/s13201-019-1102-x
10. Devanand MR, Kundapura S. Flood inundation mapping of harangi river Basin, Kodagu, using GIS techniques and HEC-RAS Model. In: *Lecture Notes in Civil Engineering*. Singapore: Springer; 2020. p. 665-678. doi: 10.1007/978-981-15-6828-2_50
11. Mishra AK, Meera MS, Nagaraju V. Exploring extreme flood events of a western state of India during monsoon season of 2019 from space. *Mausam*. 2023;75(1):245-248. doi: 10.54302/mausam.v75i1.3568
12. Das S, Das T. Flood, livelihood, and community resilience: A study from Barak Valley region of Assam in Northeast India. In: *International Handbook of Disaster Research*. Singapore: Springer; 2022. p. 1-14. doi: 10.1007/978-981-16-8800-3_63-1
13. Gogoi PP, Vinoj V, Phukon P. Role of meteorology and local orography on a flood event in the Lower Subansiri Basin and post-flood changes to land use and land cover. *Curr Sci*. 2020;118:778-785. doi: 10.18520/cs/v118/i5/778-785
14. Das K, Simhachalam A, Bora AK. *Application of Geospatial Technology in Seasonal Flood Hazard Event in Dhemaji District of Assam*. Singapore: Springer; 2022. p. 247-269. doi: 10.1007/978-3-031-15501-7_10
15. Longkumer W, Kannan H. Between floods and climate change: Revisiting the mishing community of Majuli Island, Northeast India. *Asian J Water Environ Pollut*. 2024;21(2):57-64. doi: 10.3233/ajw240022
16. Mishra AK, Meer MS, Nagaraju V. Satellite-based monitoring of recent heavy flooding over north-eastern states of India in July 2019. *Nat Hazards*. 2019;97(3):1407-1412. doi: 10.1007/s11069-019-03707-z
17. Mudashiru RB, Sabtu N, Abustan I, Balogun W. Flood hazard mapping methods: A review. *J Hydrol*. 2021;603:126846. doi: 10.1016/j.jhydrol.2021.126846
18. Sargentis GF, Iliopoulou T, Ioannidis R, *et al*. Technological advances in flood risk assessment and related operational practices since the 1970s: A case study in the Pikrodafni river of Attica. *Water*. 2025;17(1):112. doi: 10.3390/w17010112
19. Morante-Carballo F, Montalván-Burbano N,

Arias-Hidalgo M, Domínguez-Granda L, Apolo-Masache B, Carrión-Mero P. Flood models: An exploratory analysis and research trends. *Water*. 2022;14(16):2488. doi: 10.3390/w14162488
20. Das P, Dey NB. Socio-economic vulnerability in a flood affected village of Barak valley, Assam, India. *Asia Pac J Soc Sci*. 2011;3:110-123.
21. Assam Flood Handbook. *Flood Memorandum to the Ministry of Home Affairs Government of India on Assam Floods – 2022.* Government of Assam; 2022.
22. Statistical Handbook of Assam. *Statistical Handbook Assam 2021*. Directorate of Economics and Statistics Government of Assam, Guwahati; 2021.
23. Islam S, Tahir M, Parveen S. GIS-based flood susceptibility mapping of the lower Bagmati basin in Bihar, using Shannon's entropy model. *Model Earth Syst Environ*. 2022;8:1-15. doi: 10.1007/s40808-021-01283-5
24. Sarkar D, Saha S, Mondal P. GIS-based frequency ratio and Shannon's entropy techniques for flood vulnerability assessment in Patna district, Central Bihar, India. *Int J Environ Sci Technol*. 2021;19(9):8911-8932. doi: 10.1007/s13762-021-03627-1
25. Al-Hinai H, Abdalla R. Mapping coastal flood susceptible areas using Shannon's entropy model: The case of Muscat governorate, Oman. *ISPRS Int J GeoInform*. 2021;10(4):252. doi: 10.3390/ijgi10040252
26. Chowdhury S. Flash flood susceptibility mapping of North-East depression of Bangladesh using different GIS based bivariate statistical models. *Watershed Ecol Environ*. 2024;6:26-40. doi: 10.1016/j.wsee.2023.12.002
27. Arora A, Pandey M, Siddiqui MA, Hong H, Mishra VN. Spatial flood susceptibility prediction in Middle Ganga Plain: Comparison of frequency ratio and Shannon's entropy models. *Geoc Int*. 2019;36(18):2085-2116. doi: 10.1080/10106049.2019.1687594
28. Pourghasemi HR, Kariminejad N, Amiri M, *et al*. Assessing and mapping multi-hazard risk susceptibility using a machine learning technique. *Sci Rep.* 2020;10(1):3203. doi: 10.1038/s41598-020-60191-3
29. Pourghasemi HR, Rahmati O. Prediction of the landslide susceptibility: Which algorithm, which precision? *CATENA*. 2018;162:177-192. doi: 10.1016/j.catena.2017.11.022
30. Malik S, Pal SC, Arabameri A, *et al*. GIS-based statistical model for the prediction of flood hazard susceptibility. *Environ Dev Sustain*. 2021;23(11):16713-16743. doi: 10.1007/s10668-021-01377-1
31. Yesilnacar EK. *The Application of Computational Intelligence to Landslide Susceptibility Mapping in Turkey.* Australia: University of Melbourne; 2005. p. 200.
32. Horton RE. Erosional development of streams and their drainage basins; hydrophysical approach to quantitative morphology. *Geol Soc Am Bull*. 1945;56:275-370. doi: 10.1130/0016-7606(1945)56[275:EDOSAT]2.0.CO;2
33. Chetia L, Paul SK. Spatial assessment of flood susceptibility in Assam, India: A comparative study of frequency ratio and shannon's entropy models. *J Indian Soc Remote Sens*. 2024;52(2):343-358. doi: 10.1007/s12524-023-01798-7
34. Abdo HG. Evolving a total-evaluation map of flash flood hazard for hydro-prioritization based on geohydromorphometric parameters and GIS–RS manner in Al-Hussain river basin, Tartous, Syria. *Nat Hazards*. 2020;104:681-703. doi: 10.1007/s11069-020-04186-3
35. Pourali SH, Arrowsmith C, Chrisman N, Matkan AA, Mitchell D. Topography wetness index application in flood-risk-based land use planning. *Appl Spat Anal Policy*. 2014;9(1):39-54.} doi: 10.1007/s12061-014-9130-2
36. Wang N, Sun F, Demetris Koutsoyiannis, *et al*. How can changes in the human-flood distance mitigate flood fatalities and displacements? *Geophys Res Lett*. 2023;50(20):1-9. doi: 10.1029/2023gl105064
37. UNISDR. *Terminology on Disaster Risk Reduction (DRR).* Geneva, Switzerland: UNISDR; 2009b.
38. Giannakidou CH, Diakoulaki D, Memos CD. Implementing a flood vulnerability index in urban coastal areas with industrial activity. *Nat Hazards*. 2019;97(1):99-120. doi: 10.1007/s11069-019-03629-w
39. Birkmann J. Measuring vulnerability to promote disaster-resilient societies: Conceptual frameworks and definitions. In: *Measuring Vulnerability to Natural Hazards: Towards Disaster Resilient Societies*. Vol. 1. New York: United Nations University Press; 2006. p. 3-7.
40. Scheuer S, Haase D, Meyer V. Exploring multicriteria flood vulnerability by integrating economic, social and ecological dimensions of flood risk and coping capacity: From a starting point view towards an end point view of vulnerability. *Nat Hazards*. 2010;58(2):731-751. doi: 10.1007/s11069-010-9666-7
41. Sharma SV, Sarathi Roy P, Chakravarthi V, Srinivasa Rao G. Flood risk assessment using multi-criteria analysis: A case study from Kopili River Basin, Assam, India. *Geomat Nat Hazards Risk*. 2017;9(1):79-93. doi: 10.1080/19475705.2017.1408705
42. Bin L, Xu K, Pan H, Zhuang Y, Shen R. Urban flood risk assessment characterizing the relationship among hazard, exposure, and vulnerability. *Environ Sci Pollut Res*. 2023;30(36):86463-86477. doi: 10.1007/s11356-023-28578-7
43. Jaiswal R, Donahue J, Reilly MJ. Disaster risk management. In: *Ciottone's Disaster Medicine*. Netherlands: Elsevier Inc. 2016. p. 167-177. doi: 10.1016/B978-0-323-28665-7.00028-5
44. Tariq MA, Farooq R, van de Giesen N. A Critical review of flood risk management and the selection of suitable measures. *Appl Sci*. 2020;10(23):8752. doi: 10.3390/app10238752